

Assessing the Influence of Inter Tropical Discontinuity on Total Column Ozone Variation Over West Africa

Ayomide Victor Arowolo (✉ vaarowolo@gmail.com)

Federal University of Technology Akure School of Earth and Mineral Sciences <https://orcid.org/0000-0001-7881-7043>

Ayodeji Oluleye

Federal University of Technology Akure

Research Article

Keywords: Total column ozone, Inter-tropical discontinuity, Mann-Kendall, West Africa

Posted Date: December 8th, 2021

DOI: <https://doi.org/10.21203/rs.3.rs-1037029/v1>

License:  This work is licensed under a Creative Commons Attribution 4.0 International License.

[Read Full License](#)

1 **ASSESSING THE INFLUENCE OF INTER TROPICAL DISCONTINUITY ON TOTAL COLUMN OZONE**
2 **VARIATION OVER WEST AFRICA**

3 Ayomide Victor **Arowolo**^{1*} and Ayodeji **Oluleye**¹

4 ¹Department of Meteorology and Climate Science, Federal University of Technology, Akure, Nigeria.

5 Corresponding Author: Ayomide Arowolo

6 Email: vaarowolo@gmail.com

7 **ABSTRACT**

8 The focus of this study is to evaluate the influence of Intertropical Discontinuity (ITD) on the variation of
9 Total column ozone (TCO). Relevant information is supplied on the temporal and spatial variability of TCO
10 along the ITD zone, which is an important factor influencing the earth's atmosphere. Several studies over
11 the years have established the relationship and influence several atmospheric processes have on TCO.
12 However, the relationship between Intertropical discontinuity and TCO over West Africa has a gap. This
13 study tends to examine the influence ITD has on TCO variation using the West Africa region as a case
14 study. The study used Wind, ozone and dewpoint temperature data for the period between 1980-2019.
15 To assess the variability and trend over the study region, several statistical methods were used, including
16 Pearson correlation, Mann-Kendall, and linear regression model. The Mann-Kendall test shows an
17 increasing trend throughout the months over the study region. Spatial analysis also revealed that regions
18 North of the ITD has a higher concentration of TCO that the southern region of the ITD. however, ITD
19 influence was more visible during the wet month of June to August (JJA) as the highest concentration of
20 TCO was observed during this period across all latitude but more deviation was observed between latitude
21 10^oN to 18^oN, while the least occurrence is observed when ITD is at its minimum position in the month of
22 December to February (DJF). The ACRV shows that 14^oN exhibit the highest variation with a value of 4.84,
23 while the deviation is also at its highest with value of 13.65. The monthly position of ITD for Forty years
24 was also analysed to observe the monthly deviation along the ITD region forty years and the spatial
25 distribution of TCO was analysed from January to December. It's of note that during the cause of this
26 study, ozone hole which is designated by concentration less than or equal to 220DU was not recorded.
27 The highest and the lowest value of TCO is 295DU and 227DU respectively with an average range of 68DU.

28

29 *Keywords: Total column ozone, Inter-tropical discontinuity, Mann-Kendall, West Africa.*

30

31 **1. Introduction**

32 The study of ozone has been on the increase by climate researchers all over, in the past few decades, this
33 is due to the known effect and influence Ozone has on atmospheric processes which cannot be over
34 emphasized. Ozone, with the empirical formula (O₃), is a triatomic molecule composed of three oxygen
35 atoms which is mostly found in the stratosphere, where it shelters humans from the Sun's unhealthy
36 ultraviolet radiation (UV) (Akinyemi and Oladiran, 2007, Eresanya et al., 2017). its quantity in the
37 atmosphere is very small when compared with other gases. (Kondratyev and Varotsos 1996, Efstathiou et
38 al. 1998). O₃ is an essential chemical element of the atmosphere that affects the energy budget and
39 chemistry of the atmosphere along with air quality and global climate change (Duenas et al., 2004;
40 Ahammed et al., 2006; Lin et al., 2008; Nishanth et al., 2014). This gas is mostly created by photochemical
41 processes, although it may also be produced when a soothing electric discharge passes over oxygen.
42 (Akinyemi, 2010). As a result, during electric storms, it can be produced in exceptionally small quantities.
43 Because of its capacity to absorb both incoming solar UV and portion of visible light, as well as re-emit
44 and absorb outgoing terrestrial infrared (IR) radiation, ozone has been acknowledged being one of the
45 most prominent radiative gases in the stratosphere and upper troposphere. As a result, variations in ozone
46 concentrations have an effect on climate, which is dependent on the altitudes at which the changes occur.
47 (Bojkov and Fioletov, 1995; Orsolini et al., 1998).

48 Transport mechanisms are the primary source of changes in the lower atmosphere. Ozone in the lower
49 stratosphere serves as a tracer of atmospheric movements as a result of this activity. The dynamics of
50 motion in the atmosphere are linked to this motion. The stratosphere's transport and wind motion are
51 linked to that of the troposphere; For instance, at the tropopause, ascending air is carried into the
52 stratosphere and expelled from the column at higher heights above a tropospheric high-pressure system.
53 Because the ozone-mixing ratio in the lower stratosphere rises with altitude, the air entering this column
54 has less ozone than the air leaving it. The quantity of ozone in the column drops as a result. As it advances,
55 this high-pressure system drags the low-ozone column after it. This explains why high-pressure systems
56 are connected to reduced stratospheric ozone levels.

57 A low-pressure system has the opposite effect, causing a rise in ozone levels (Cordero and Forster, 2006).
58 The tropical region produces the maximum stratospheric ozone, which slowly disperses towards the mid-
59 latitude and polar regions due to the effect of Brewer-Dobson circulation. In this circulation, Tropical air
60 ascends from the troposphere to the stratosphere, moving towards higher latitudes, and then descends
61 into the troposphere around mid-latitude while in the stratosphere over the polar area in this cycle.

62 (Brewer, 1949 and Butchart 2014). The highest concentration of ozone over the mid-latitude and polar
63 regions is due to this phenomenon, as opposed to the tropical area. The majority of ozone research is
64 conducted in the mid-latitude and polar areas, where ozone depletion is more severe than it is in the
65 tropics. (Farman et al., 1985). The variations in stratospheric ozone are sensitive to solar activity,
66 atmospheric circulation and the angle of the sun's radiation.

67 The convergence of the trade winds of the two hemispheres is the fundamental description of Inter-
68 Tropical Discontinuity (ITD) (southern and Northern). Low pressure, rising motion, clouds, and
69 precipitation characterize this system. In other words, the onset, retreat, and length of the rainy season in
70 the tropical area are governed by two air masses meeting at a slanting surface with a sun synchronous
71 movement.

72 During the months of March and April, ITD spreads from the Gulf of Guinea coast to the north. This signifies
73 the beginning of the first rainy season along the Guinean coast south of 100°N. (Sultan and Janicot,2003).
74 The ITD continues to spread inland over the next few months (Lothon et al., 2008), reaching its
75 northernmost climatological location in July and August at around 210N. (Sultan et al., 2007).

76 The ITD location does not change over several months, but it is influenced by a variety of processes at
77 different time scales, ranging from daily low-level jets (Flamant et al., 2009) to multi-day pulsations with
78 cycles of approximately 5 days (Couvreur et al., 2010). The ITD is positioned in the equatorial trough, a
79 continuous low-pressure region that marks the geographic equator. Surface trade winds converge to
80 generate a zone of heightened mean convection, cloudiness, and precipitation, transporting heat and
81 moisture from surface evaporation and sensible heating.

82

83 **2.0 Data and methods**

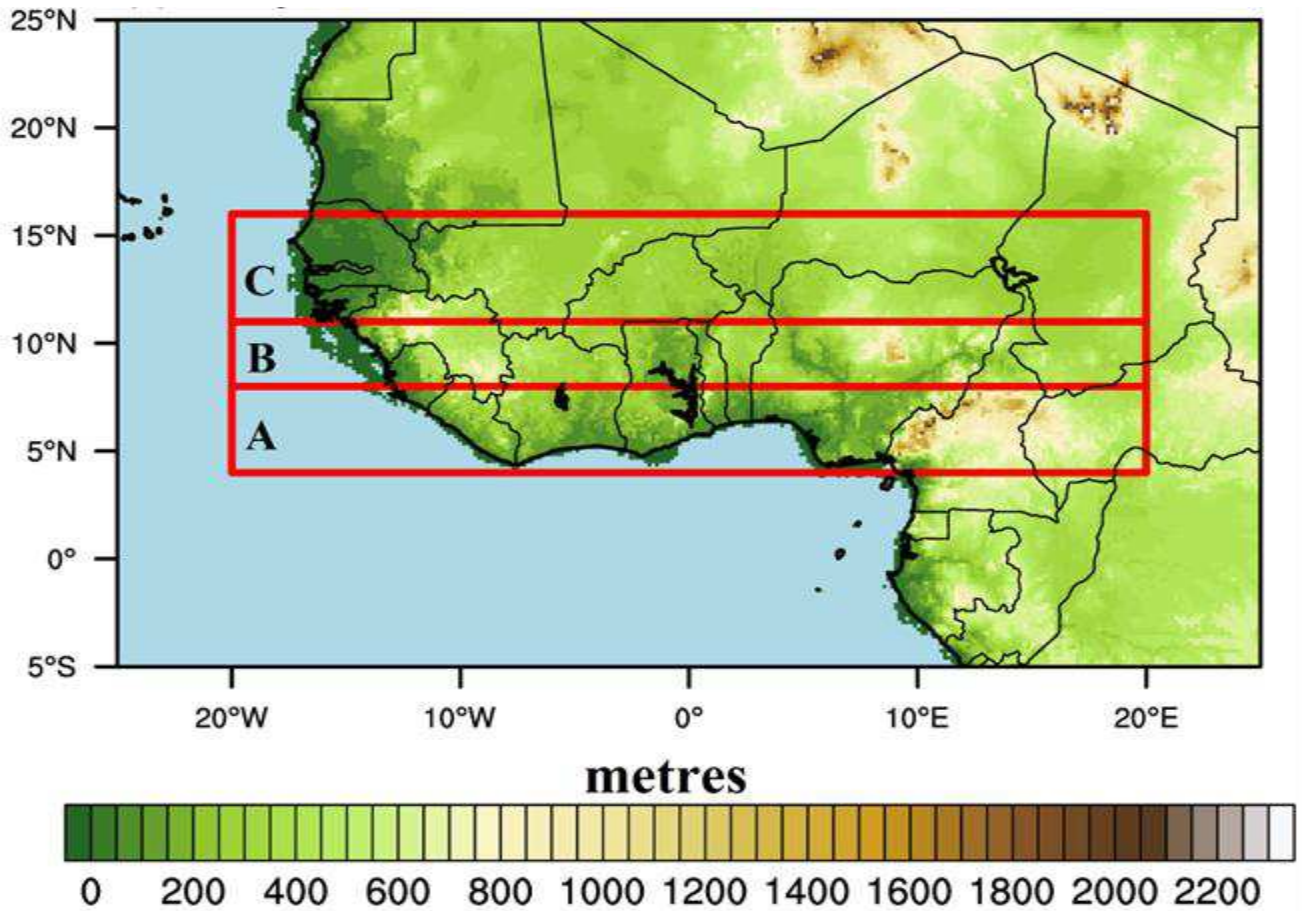
84 **2.1 Description of the area of study**

85 This research focuses on the West Africa subcontinent, which is formed from the Africa continent. As
86 indicated in Figure 1, the area spans latitudes 00S to 25ON and longitudes 20OW to 20OE.

87 Geographically, the Gulf of Guinea forms the southern border, while Mauritania, Mali, and Niger form
88 the northern border. Its eastern and western boundaries are Mount Cameroun and the Atlantic Ocean,
89 respectively. Nigeria, Benin, Ghana, Niger, Togo, Cape Verde, Senegal, Gambia, Guinea-Conakry, Ivory
90 Coast, Guinea Bissau, Liberia, Mali, Mauritania, Sierra Leone, and Burkina Faso are among the 16 nations
91 that make up the region, which spans over 5 million square kilometres. The climatology of the West

92 Africa region is governed by the Inter-Tropical Discontinuity's latitudinal movement (which is a north-
93 south movement), and the three main climatic zones are: Guinea coast (4ON – 8ON), Savannah (8ON –
94 11ON), and Sahel (11 O N – 16 ON) according to the classifications defined in (Omotosho and Abiodun,
95 2007; Akinsanola et al., 2015). The Guinea coast is the southernmost point of the Atlantic Ocean, and it
96 has a sub-humid climate with annual rainfall ranging between 1250 and 5000 mm. This is the realm of
97 the deciduous or semi-deciduous forest that is moist and dry throughout the year.

98



99

100 **Fig. 1** Map of the study area, showing the western boundaries

101 The savannah zone is a semi-arid region with annual rainfall ranging from 750 to 1250 millimetres. The
102 Sahel zone, which spans along the northern borders of Mauritania, Mali, and Niger, is characterized by a
103 single rainfall peak (June to September) with an annual rainfall of approximately 750mm. The average
104 annual temperature is usually over 18 degrees Celsius. The mean annual temperature in areas within 10
105 degrees north of the equator is roughly 26°C, with a range of 1.7–2.8°C and a diurnal range of 5.6–8.3°C.
106 Even though the yearly range is 9°C and the diurnal range is 14° to 17°C, monthly mean *temperatures*

107 between latitudes 10°N and the southern section of the Sahara can reach 30°C. The average yearly
108 temperature in the middle Sahara varies between 10°C and 35°C (Food and Agriculture Organization,
109 2001).

110 **2.2 Data Acquisition and Analysis**

111 Three datasets were utilized in this study: total column ozone, zonal wind, and dew point temperature.
112 The total column ozone dataset was derived from MERRA-2, the most recent global atmospheric
113 reanalysis for the satellite era generated by NASA's Global Modelling and Assimilation Office (GMAO)
114 using the Goddard Earth Observing System Model (GEOS) version 5.12.4. Zonal wind and dewpoint
115 Temperature was obtained from ERA-Interim which is produced by the European Centre for Medium
116 Range Weather Forecast (ECMWF). All data was obtained for the period between January 1980 to
117 December 2019 at 25km x 25km resolution.

118 In order to delineate the position of Inter-Tropical Discontinuity (ITD) over the study region, the monthly
119 mean convergence of the zonal winds for the study period was plotted and the line of vector discontinuity
120 was derived. The delineated position was assessed with Monthly analysis of Spatio-Temporal variation of
121 total column ozone. This was carried out in order to determine the spatial distribution and temporal
122 variation along the inter-tropical discontinuity.

123 Long term variation of Total Column Ozone is represented by a linear regression equation given as;

$$124 \quad Y = bx + c \quad (1)$$

125 Where x is the monthly value of Total Column Ozone,

126 And Y is the monthly mean of Total Column Ozone;

127 where b and c are constants of regression. An equation which describes the temporal change of TCO
128 concentration. The equation for the trend is therefore given as:

129

$$130 \quad \text{Trend} = \frac{b \times 12 \times 10}{\text{AvGTCO} \times 100} \quad (2)$$

131

132 Also, the annual coefficient of relative variation (ACRV) is given as;

133

$$134 \quad \text{ACRV} = \frac{\text{ANNUAL SD}}{\text{ANNUAL MEAN}} \times 100 \quad (3)$$

135

136 Where SD= standard deviation.

137 Where x is the observed TCO, and \bar{x} and S_x are the mean and standard deviation of TCO.

138 Mann-Kendall test (Mk) (Mann 1945; Kendall 1975; Wang et al., 2005) was also used for the trend analysis.
 139 This was used to determine discontinuities due to inhomogeneous time succession. It is unique as it does
 140 not need presumptions analogous to data distribution. (Mondal et al., 2012). This makes it widely
 141 acceptable for trend analysis. (Ilori and Ajayi, 2020; Khan et al., 2020; Jonah et al., 2021) Mk statistic can
 142 be described as:

$$143 \quad K = \sum_{i=1}^n \sum_{j=1}^{i-1} \text{sign}(x_i - x_j) \quad (4)$$

144 Where x_i and x_j are the value of the sequential generic data, n is the data total length, while $\text{sign}(x_i - x_j)$
 145 can be defined as;

$$146 \quad \text{Sign}(x_i - x_j) = \begin{cases} 1, & \text{if}(x_i - x_j) > 0 \\ 0, & \text{if}(x_i - x_j) = 0 \\ -1 & \text{if}(x_i - x_j) < 0 \end{cases} \quad (5)$$

147
 148
 149 The variance $\text{Var}(S)$ was calculated as follows when S statistic is approximately distributed with the $E(S)$
 150 mean:

$$151 \quad E(S) = 0, \quad (6)$$

$$152 \quad \{n(n-1)(2n+5) - \sum_t t(t-1)(2t+5)\} \quad (7)$$

153
 154 Where t is any given tie extent, $\sum t$ represents the summation of all values of the tie number, while n
 155 denotes length of the series. The Z standardized statistics for the test can then be evaluated using the
 156 equation below:

$$157 \quad Z = \begin{cases} -1, & \text{if } K < 0 \\ 0, & \text{if } K = 0 \\ \frac{S+1}{\sqrt{\text{Var}(S)}} & \text{if } K > 0 \end{cases} \quad (8)$$

158 When a dataset of n variables is randomly distributed independently without trend and ordering is equally
 159 likely, the null (H_0) hypothesis is accepted. The absolute value of Z (test statistic) is then compared with
 160 the value of $Z\left(1 - \frac{p}{2}\right)$ at p level of significance obtained from the table to reject or accept the H_0
 161 hypothesis.

162
 163

164 **Data Description**

DATA	SPATIAL RESOLUTION	TEMPORAL RESOLUTION	SOURCES	UNITS
Total column Ozone	0.25 x 0.25	Monthly	GIOVANNI	Du
Dew Point Temperature	0.25 x 0.25	Monthly	ERA Interim	Kelvin
Uwind, Vwind	0.25 x 0.25	Monthly	ERA Interim	m/s

165 **Table 1:** Data source, type and description.

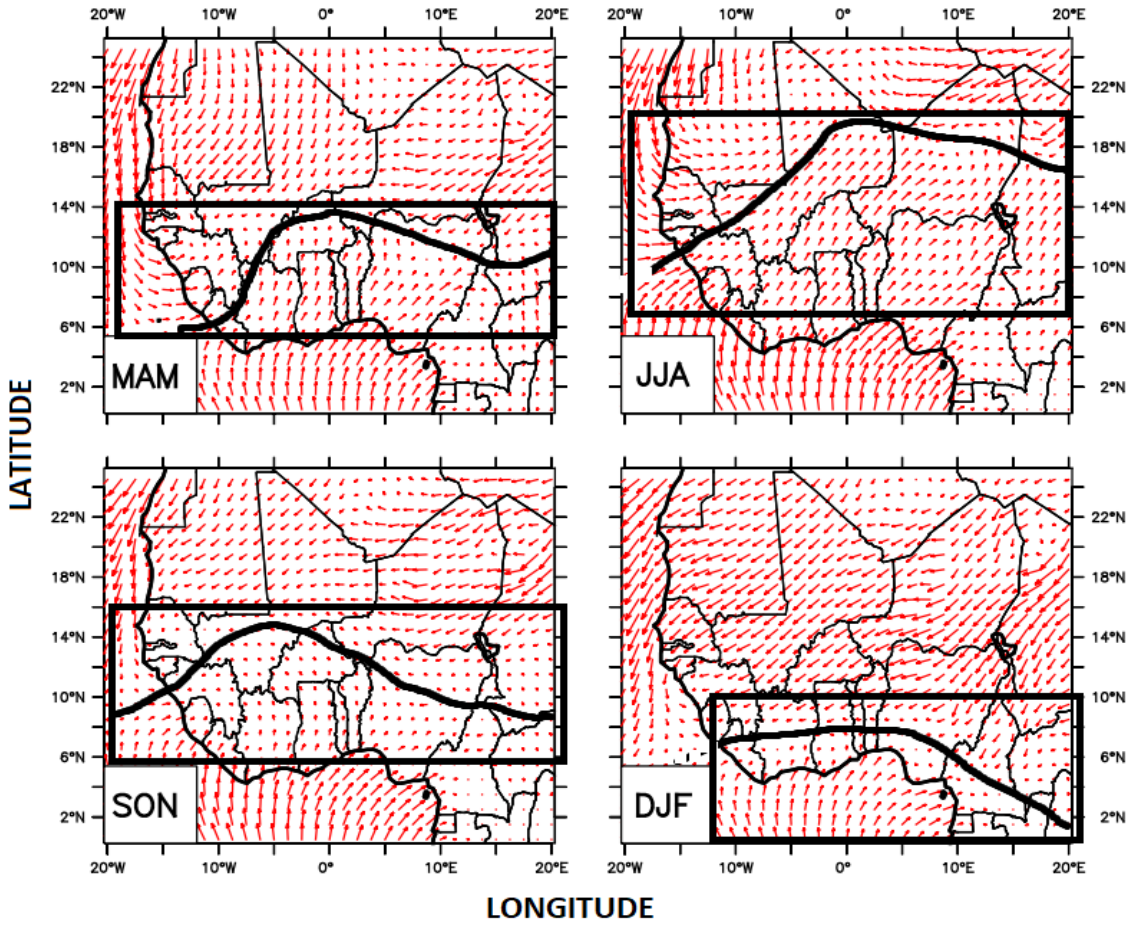
166 The zonal and meridional wind data were downloaded at standard height of 10m above the ground level

167

168 **RESULTS AND DISCUSION**

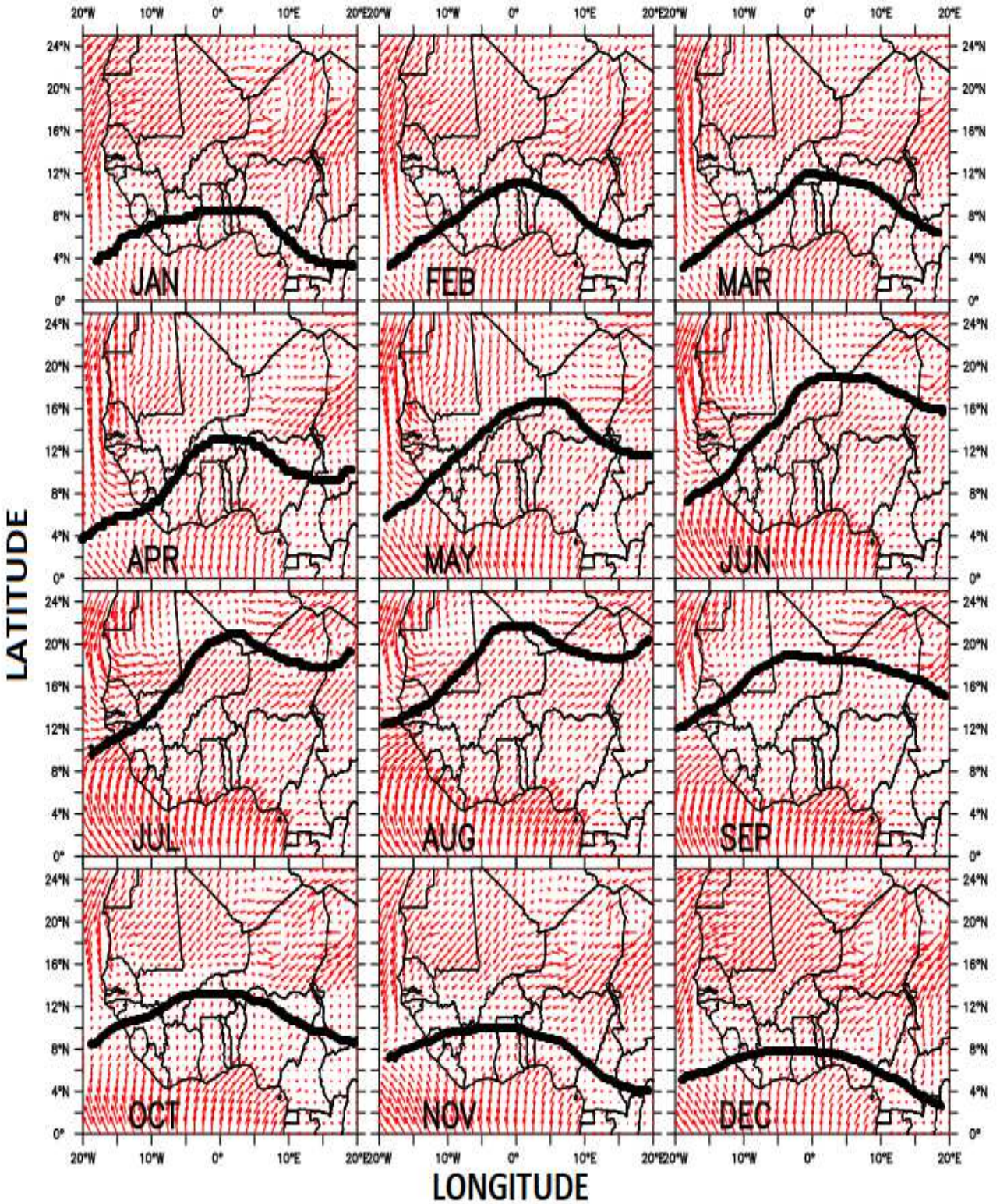
169 The Inter-Tropical Discontinuity over land is a low-pressure system generated when the northeast and
 170 southwest trade winds meet near the Earth's equator in West Africa. It's important to stress that the ITD
 171 is a zone rather than a demarcation line; however, the Inter-Tropical Front (ITF), which is the same as the
 172 ITD's northernmost boundary, is defined as a line. ITD which is generally used to represent the boundary
 173 between the dry north winds and the warm humid winds to the south (Griffiths & Soliman, 1972; Kalu,
 174 1977; Dubief, 1979; Adeyefa et al., 1995).

175 The convergence points of the northeast and the southwest wind streamlines was considered to be the
 176 average surface position of the ITD over the region on daily basis.



177

178 **Fig. 2** Seasonal position of ITD over the study region



179

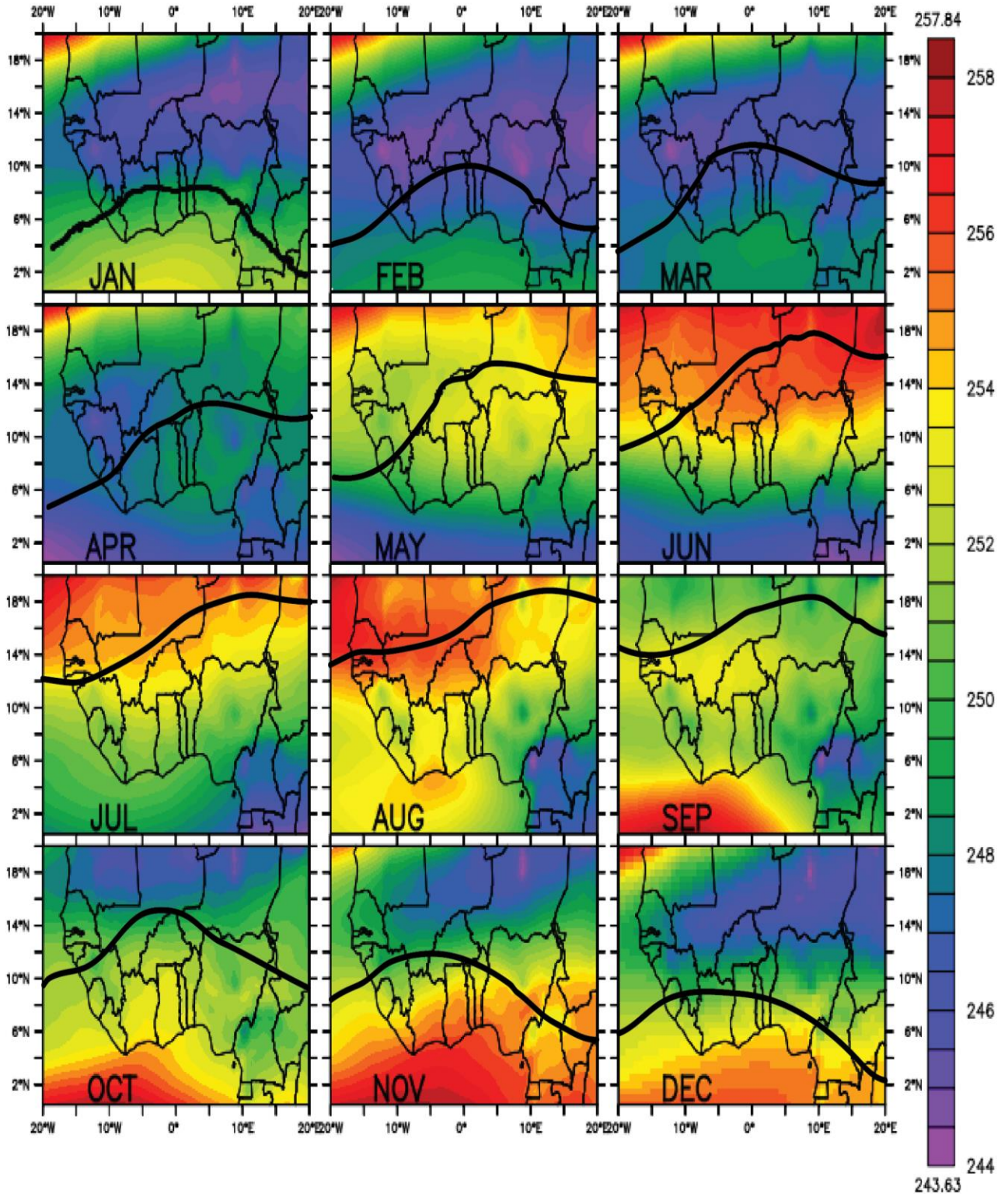
180 **Fig. 3** Monthly mean position of ITD from January to December

181 The figure 3 shows the monthly mean position of ITD for a period of 10 years (2010-2019). While figure 2
182 shows the seasonal position of ITD for a period between 1980 to 2019. ITD can be observed to be between
183 2-22⁰N for the monthly position and between 2-20⁰N for the seasonal position. The surface wind
184 convergence and dew-point temperature of 15⁰C was used to delineate this position. Using surface wind
185 convergence to delineate the position of ITD over West Africa is a widely accepted method as it takes into
186 consideration the surface level wind convergence which denotes the meeting point of two airmasses.
187 (Odekunle, 2010; Lele and Lamb, 2010; Oluleye and Jimoh., 2017) The northernmost position is seen to
188 be at the northern boundary of West Africa at 22⁰N. The black continuous line shows the position of ITD
189 at each month over the region, as illustrated in figure 2 and 3.

190 Wind direction and dewpoint temperature for each month was averaged through a span of 10 years and
191 the monthly and seasonal mean value was derived over the study area. The most significant movement of
192 ITD was observed at June, July, August (JJA) with its northernmost position at 20⁰N, while it extended from
193 10⁰N. While the season with the least variation was observed at MAM (March, April, May) which span
194 between 6-14⁰N, similar observation was also made at SON (September, October, November). West Africa
195 has two major distinct seasons, namely wet and dry season. Wet season ranges from JJA and SON, while
196 dry season range from MAM and DJF. These dry months has the lowest propagation of ITD, while
197 significant observation was recorded during the wet months as in JJA and SON.

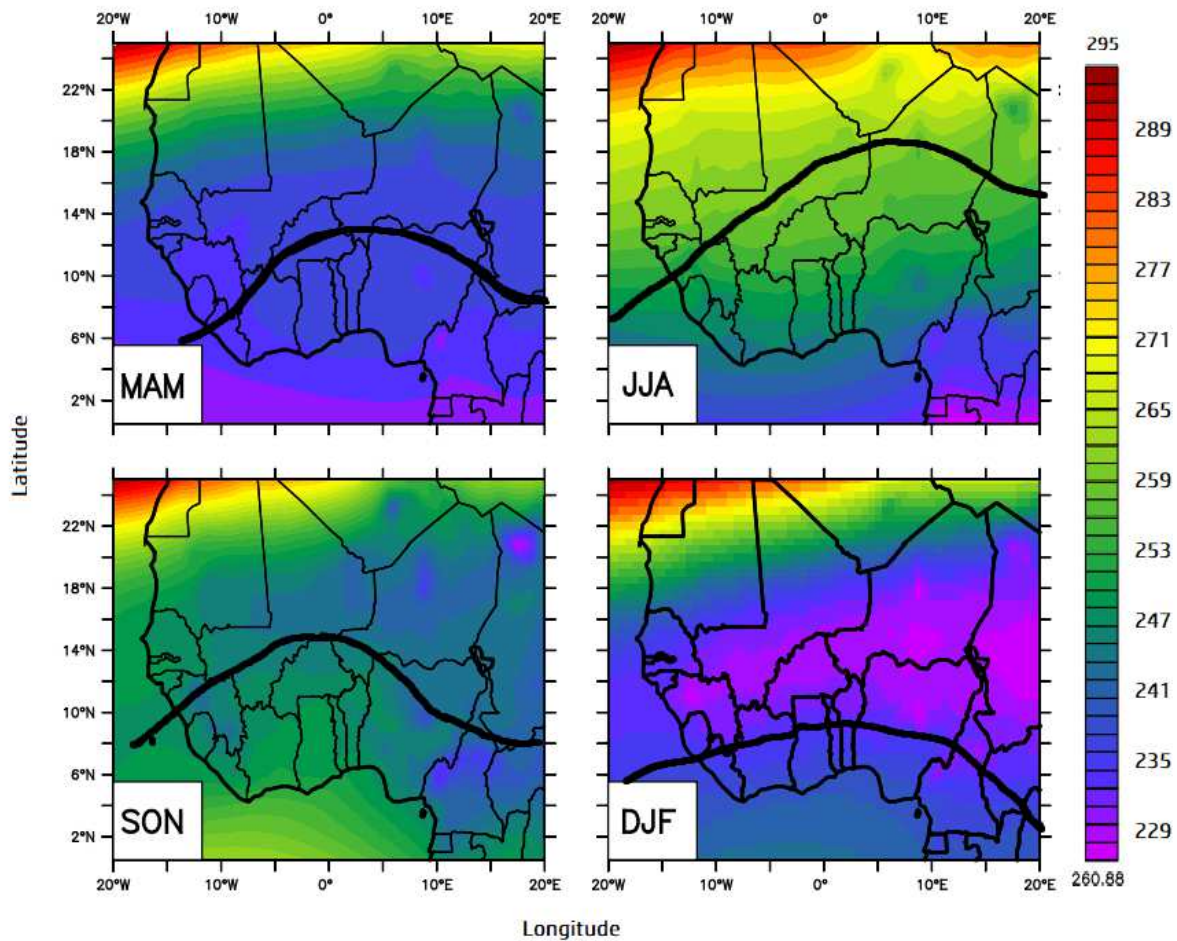
198 The positions of ITD in this study can be seen to be symmetrical with rainfall pattern over West Africa, as
199 ITD is the major indicator of rainfall system as observed by kalita et al., 2011.

200
201
202



203

204 **Fig. 4** Monthly distribution of Total column ozone over the West Africa Region, For a period between
 205 2000 to 2019.



206
 207 **Fig. 5** Seasonal position of ITD with spatial distribution of Total column ozone over West Africa from a
 208 period between 1980 to 2019.

209 Figure 5 depicts TCO range to be between 227-295 DU from January to December which shows a
 210 difference of 68 DU. The black line shows the position of ITD over the region for each month as previously
 211 delineated and observed in figure 2 and 3. From figure 4 ITD position over West Africa in the dry months
 212 shows that regions south of the ITD which is dominated by the southwest trade wind exhibit a higher
 213 concentration of TCO while region north of the ITD which is dominated by northeast trade wind has a
 214 lower concentration between depicted between latitude 8-14⁰N, this phenomenon may be attributed to
 215 the dominance of the Northeast trade wind over the region. The ITD trough itself is seen to have a
 216 considerable low concentration of TCO which is considered to be averagely low in the dry months. As also
 217 observed in figure 5. In DJF, north easterly wind dominates most of West Africa region as indicated, also
 218 the concentration of TCO over DJF is seen to be at its lowest. The ITD position slants, propagating along
 219 the West African coast lines from latitude 9⁰N to 2⁰N across the West to east region of West Africa,

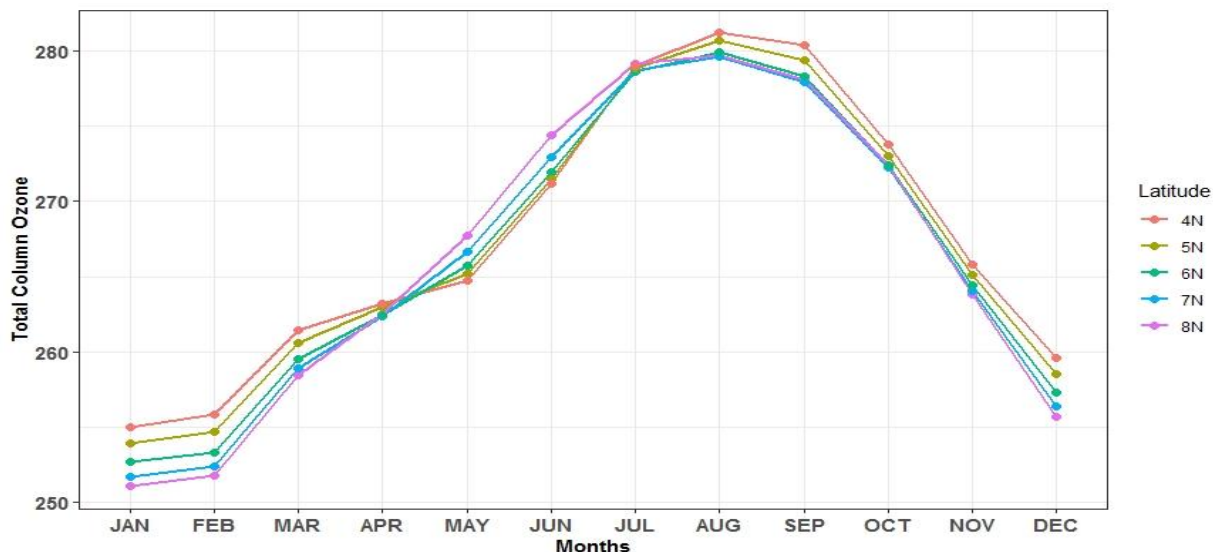
220 indicating a dry period of the year when an observation at the wind system for the month of April indicates
221 that southwesterlies have gained momentum over the northeasterlies this is observed as the ITD position
222 is seen to be located at 13°N and this also signals the beginning of rainfall for most West African region.
223 In February also, the concentration is also low along the ITD trough, but with a considerably higher value
224 than TCO concentration in January. In comparison, TCO has a higher concentration in January than
225 February. Also in March, the ITD position is seen to have moved northward by 2°N, region of the ITD
226 trough is also observed to have a lower concentration of TCO than the surrounding region. April and May
227 also have the same low concentration along the ITD trough.

228 JJA have different condition, the concentration of TCO in this month is relatively higher than other months,
229 these months are also months when ITD is at its peak and the southwesterlies wind are dominant which
230 is also regarded as the rain peak over west Africa.

231 As the moist south westerly wind stabilizes over the region in JJA when ITD is reaching its northernmost
232 position as observed in figure 2 and 3, ozone concentration is seen to significantly increase in
233 concentration and propagation of ITD is observed to be at its peak. however, in September when ITD
234 begins to retreat, also marks the beginning of ozone decrement which wind up in returning to January
235 situation as the dry north easterly wind, once again, takes over the region in December. This illusive
236 transition of ITD corresponding changes in ozone concentration during the course of the year may be a
237 factor that makes weather activity most influencing factor, controlling TCO in West Africa as also observed
238 by Oluleye and Okogbue, 2013.

239 The totality of West Africa generally has a higher concentration of TCO in the month of JJA. It is also
240 observed that ITD region maintained it lower concentration while south of ITD has the highest
241 concentration of TCO. The trend also increased progressively from January and peaked at September,
242 which is also denoted as the ITD peak, and starts decreasing from October through February as previously
243 explained. In a recent study by Nishanth et al., 2021, similar observation was made over India which share
244 the same regional characteristics as west Africa as it is also a tropical region, he however attributed these
245 changes to some other meteorological variables. In a model study by (Haigh, 1994) revealed that a 1%
246 increase in Ultra-violet (UV) radiation at the maximum of a solar cycle will generate a 2% increase in ozone
247 concentrations in the stratosphere. The results from this study agrees with a study by Nishanth et al.,
248 2021, where he also observed significant increase in TCO concentration in months of June, July and August
249 which also has the highest concentration in this study, which he attributed to south-West monsoon over
250 the delineated locations.

251 **TCO Variation across Latitudes**



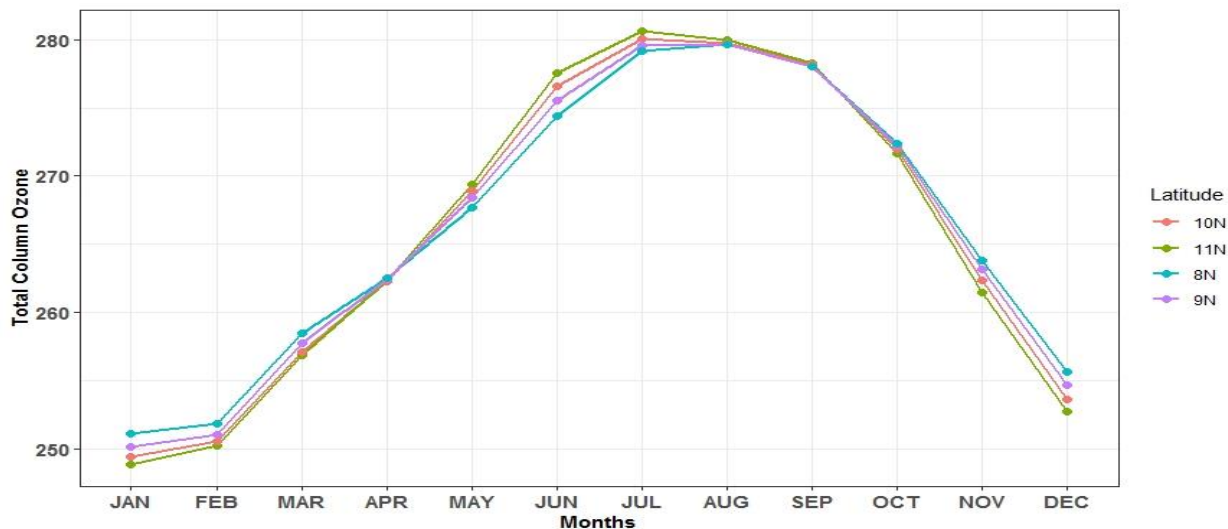
252 **Fig. 6** Monthly variation of Total column ozone over the Guinea-Coast

253 TCO trend over the guinea coast established a relationship between ITD and Ozone as shown in figure 6.
 254 The guinea coast is a region of maximum precipitation, when compared to the Savannah and Sahel, it lies
 255 between 4-8⁰N. The maximum concentration of TCO occurred in August. while July, August, September is
 256 observed to have the highest concentration of TCO over the guinea coast. This feature is most likely linked
 257 to increase rainfall, cloud cover, large wind speed and lower atmospheric temperature which are the
 258 features of wet season in the guinea coast.

259 During the month of January, February, March and December, which has notably the lowest concentration
 260 of TCO, this may also be linked to atmospheric phenomenon associated with the dry period which include,
 261 more sunshine hours, high temperature, low humidity, sparse cloud cover. The highest concentration of
 262 TCO occurred in July over the guinea coast, while the minimum concentration occurred at January,
 263 February and December, which is associated with little or no rainfall over the West Africa region. Generally,
 264 High concentration were observed between June to September, with concentration between 270DU-
 265 282DU, which can be attributed to increased monsoon rainfall. While low concentration was observed
 266 between January-March, which signals the Northward advancement of ITD and November-December,
 267 which also signals the retreat of ITD over West Africa.

268 Also, across the latitude, lower latitude is observed to have a higher concentration of TCO, while higher
 269 latitude is observed to have a lesser concentration as seen in figure 6, the study of the trend between
 270 latitude 4⁰N and 8⁰N revealed the variability between the latitudes. As they all increase steadily between

271 January and march, interchanging positions at April, as it is observed that concentration at 8°N is now
 272 higher than TCO concentration at 4°N. From May through July, this progression is continued before
 273 reverting to the initial position. The presence of ITD, which influences the concentration of ozone across
 274 this latitude, is responsible for this divergence.



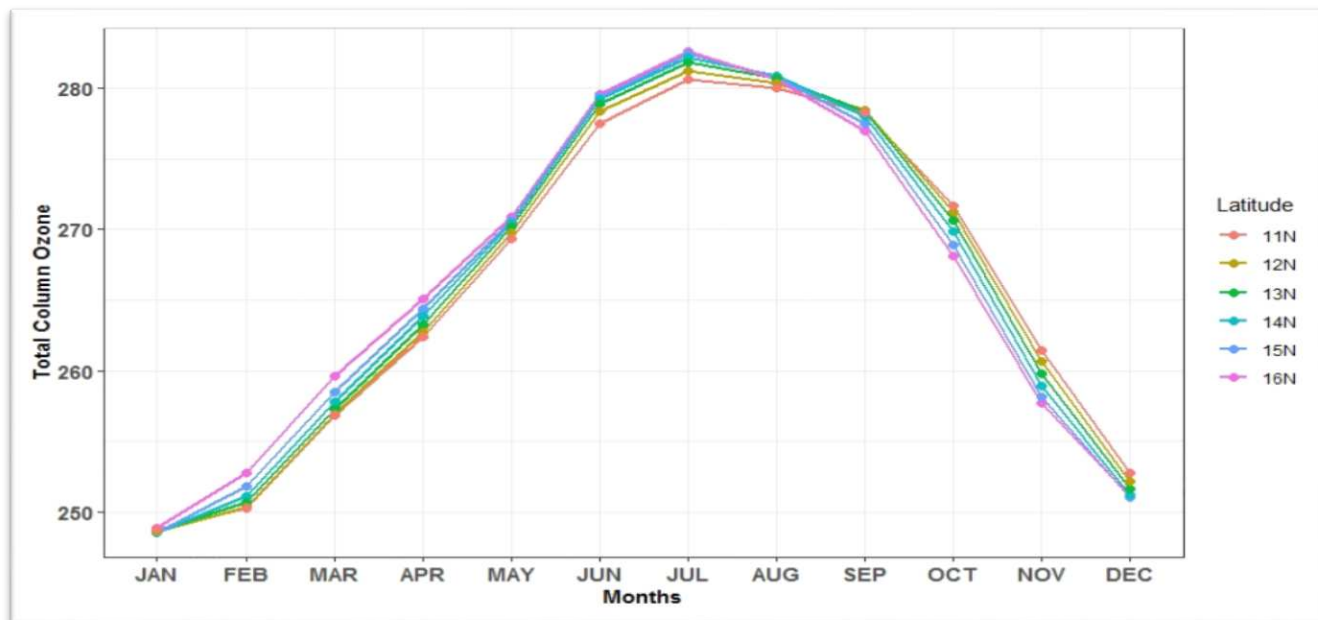
275

276 **Fig. 7** Monthly variation of Total column Ozone over the Savannah

277 Figure 7 further describe TCO variation across latitude as observed over the savannah region. Savannah
 278 region is situated between latitude 8-11°N, it has lesser precipitation when compared to the guinea coast.
 279 Maximum concentration is also at July with a TCO concentration of 280DU at 11°N as compared to Guinea
 280 coast which peaked at august and a TCO peak of 282DU. Over the savannah region, June, July, august and
 281 September has the highest concentration with a difference of less than 5DU as compared to the Guinea
 282 coast which has a difference of about 10DU, while DJF still maintained the lowest concentration over the
 283 region.

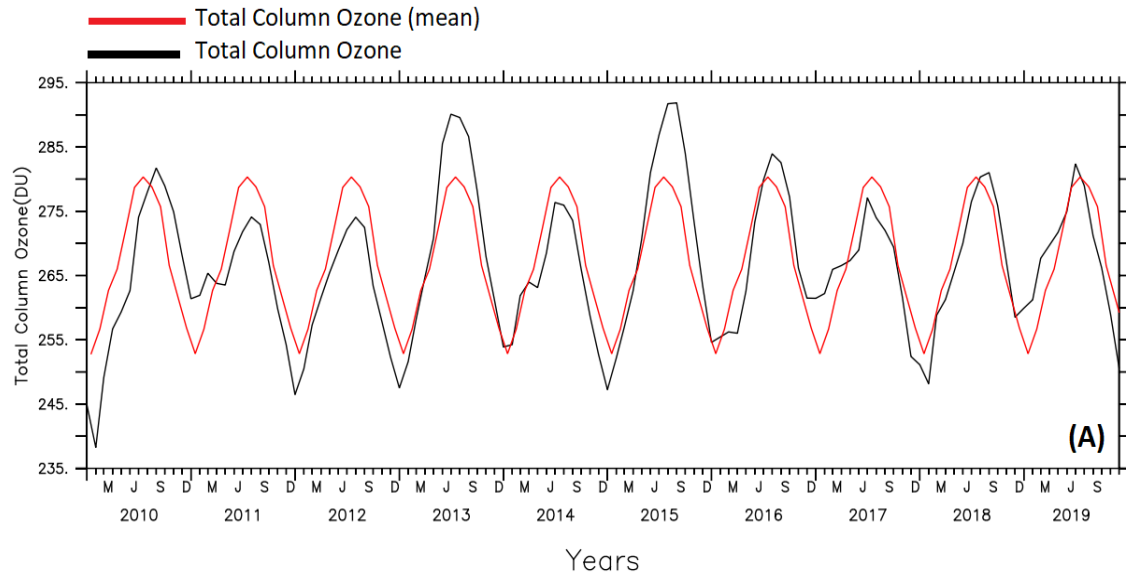
284 This region exhibits a significant difference from the Guinea coast has observed in January, latitude 8°N
 285 has the highest concentration of TCO till April, which signals the movement of ITD to this latitudinal
 286 position. The concentration drops to being the lowest at April. The concentration is reversed from 11-
 287 8°N throughout till TCO peak at July as opposed August of the previous zone. Then at august, the
 288 latitudinal position concentration is maintained till October which is also revert back the TCO
 289 concentration at each latitude to the initial position. These changes can also be attributed to the
 290 presence of ITD at this region in the month such as January, April, August and October.

291 The savannah region is observed to be less concentrated than the guinea coast. As it has much lower
292 concentration in December, January, February progressively till it peaked at July when compared to
293 Guinea coast.



294 **Fig. 8** Monthly variation of Total column Ozone over the Sahel

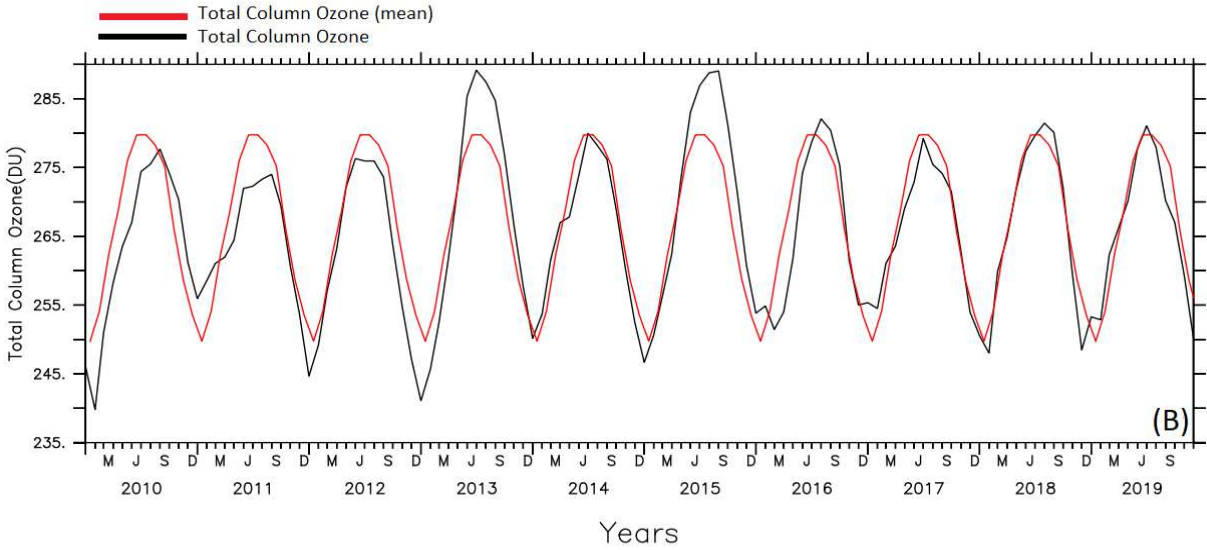
295 While over the Sahel, which is regarded as the driest region which has the least impact of ITD. TCO is
296 observed to have the same value for January across the six Sahelian latitudinal region. It is also observed
297 to peak at July as same with the savannah region. However, latitudinal positions are maintained till august,
298 which over Sahel region signifies the beginning of the dry season. This also correlated with the position of
299 ITD as observed in figure 4, over the months and across latitudinal regions shows that June, July, August
300 and September are months were ITD position is northernmost.



301

302 **Fig. 9** Annual Trend of TCO Over the Guinea Region

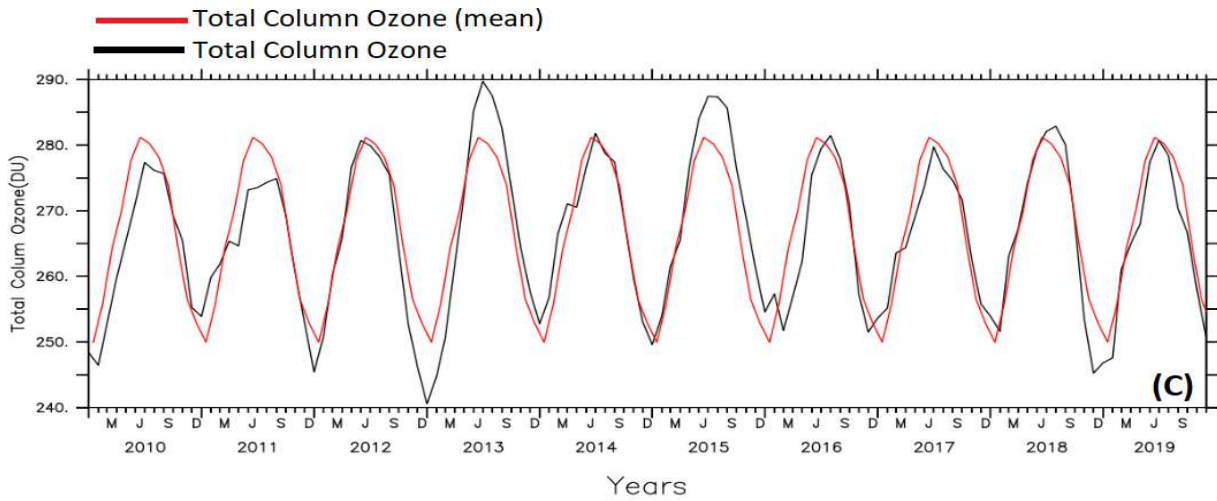
303 Figure 9 shows the annual and mean trend of TCO over the guinea coast. The guinea coast region which
 304 has the presence of ITD almost throughout the year is observed to have a significant minimum value in
 305 the month of February in 2010 and maximum at August in 2015. While the mean range is between 253
 306 and 280 DU over the Guinea coast. The minimum and maximum value for TCO in this region is 238 and
 307 292 respectively. The trend also indicates a pattern along which ITD propagates. From
 308 January/December to July/august, there seems to be a significant progressive increment in the value of
 309 TCO across the study period and a decrease in the concentration from July/August to
 310 December/January. These establishes a relationship between ITD movements across the months and
 311 Total column ozone concentration along the region. the lowest concentration of TCO was observed at
 312 February 2010 while the highest concentration was observed at July/August 2015.



313

314 **Fig. 10** Annual Trend of TCO over the savannah region

315 Figure 10 shows annual and mean trend of TCO over the savannah region. Which is located between
 316 latitude 8-11°N. the trend is similar to the trend over the Guinea coast but of lower TCO concentration,
 317 with a minimum of 240DU and a maximum concentration of 289DU, with a difference of 49DU, from the
 318 minimum concentration in January/December to the maximum concentration in July/august and also a
 319 mean minimum value of 250DU and mean maximum concentration of 280DU, with a mean difference of
 320 30DU. the lowest concentration of TCO was observed at February 2010 while the highest concentration
 321 was observed at June 2013.



322

323 **Fig. 11** Annual Trend of TCO over the Sahel region

324 Figure 11 shows annual and mean trend of TCO over the Sahelian region, which is located between latitude
325 12-16°N. the trend is similar to the trend over both the Guinea coast and the savanna region, having also
326 the same lower TCO concentration with the savannah region, with a minimum of 240DU and a maximum
327 concentration of 290DU, with a difference of 50DU, also with a minimum concentration in
328 January/December to the maximum concentration in July/August and also a mean value of 250DU and
329 maximum concentration of 282DU, with a mean difference of 30DU. The major difference observed
330 between savanna and Sahel region is the shift in months of lower concentration of ozone. It occurs over
331 the savanna region majorly in November/December, while over the Sahelian region, lowest occurrence
332 was observed in December/January. The lowest concentration of TCO was observed at December 2012
333 while the highest concentration was observed at June 2013.

334 In the year 2013 and 2015, in the month of June/July respectively, there is observed to be a significant
335 increase in concentration of TCO, which may be attributed to factors other than the influence of ITD,
336 similar observation was also made in the Guinea coast and savannah region.

337 Figure 12-14 shows the regression trend at each latitude from 20°N-4°N. From 20°N-4°N, an increase in
338 the variation of TCO is observed as the slope of the trend is positive. With the exception of 18°N and
339 19°N which shows a negative trend/year. Throughout higher latitude, TCO seems to have its maximum
340 concentration to be at 2013 from 20°N-12°N while from 11°N the maximum concentration also extends
341 to 2014 making it a dual peak this is reflected as the coefficient of the slope at this region increases.
342 Similar observation was made by Nishanth et al., 2021 which he attributed to latitudinal variation he
343 also noted that changes in wind pattern influence changes in spatial and Temporal distribution of TCO.
344 Large inter annual variability of TCO concentration was also observed which can be attributed to
345 variation in tropopause height, air circulation changes, changes in anthropogenic concentration and
346 other atmospheric factors.

347

348

349

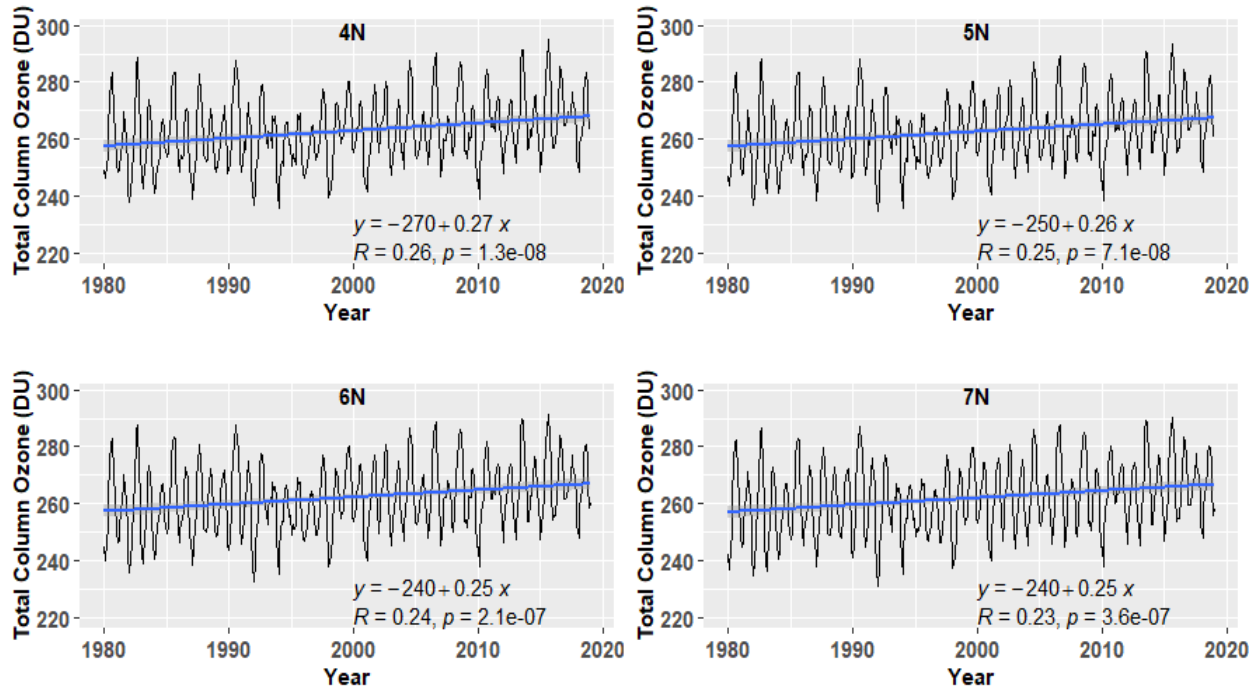
350

351

352

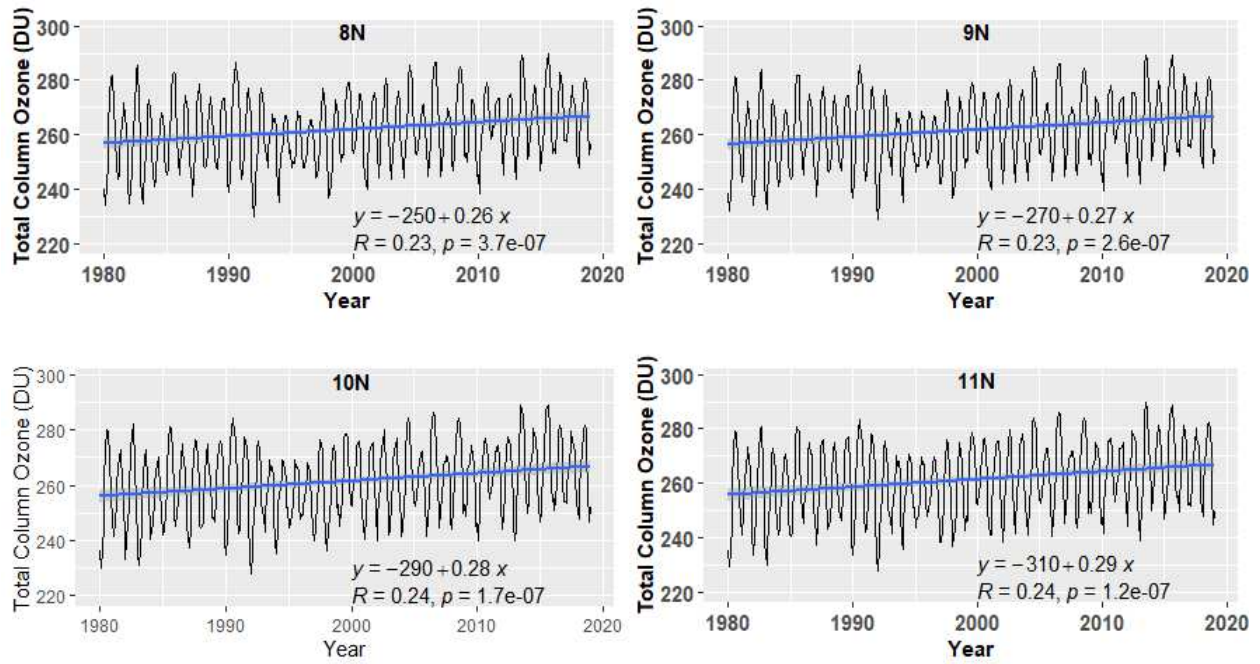
353

354 Latitudinal variation with regression trend from 1980-2019



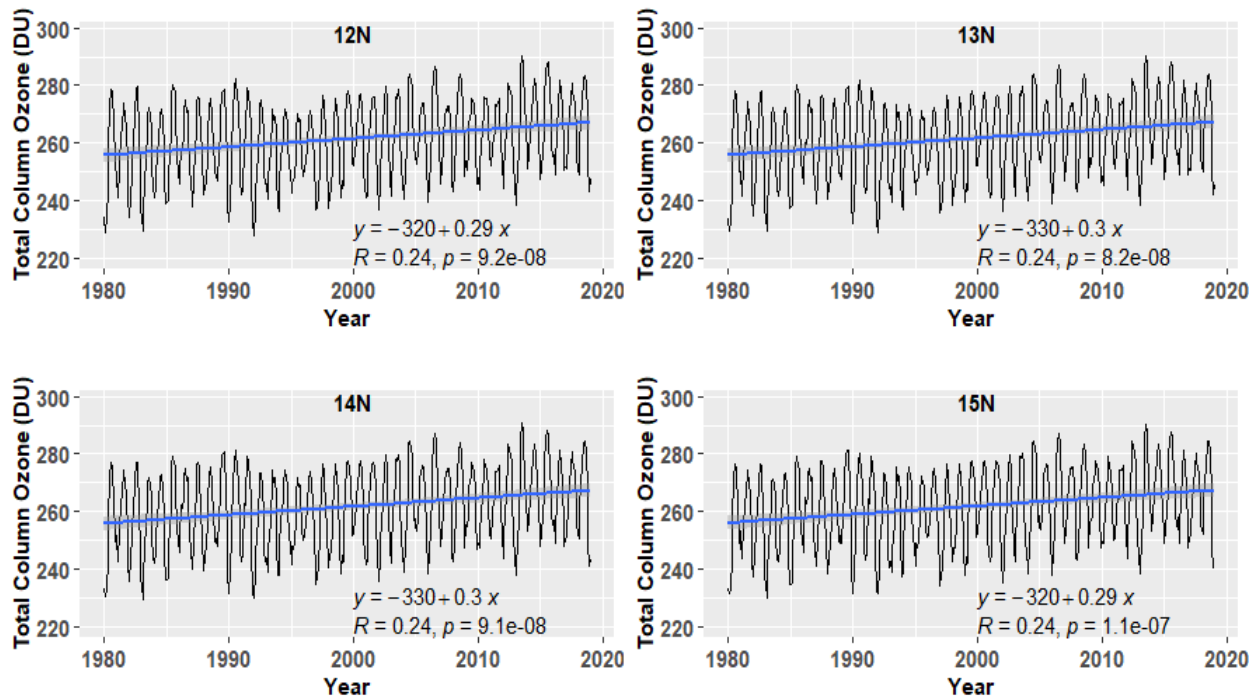
355

356 Fig. 12 Variation from 4-7⁰N



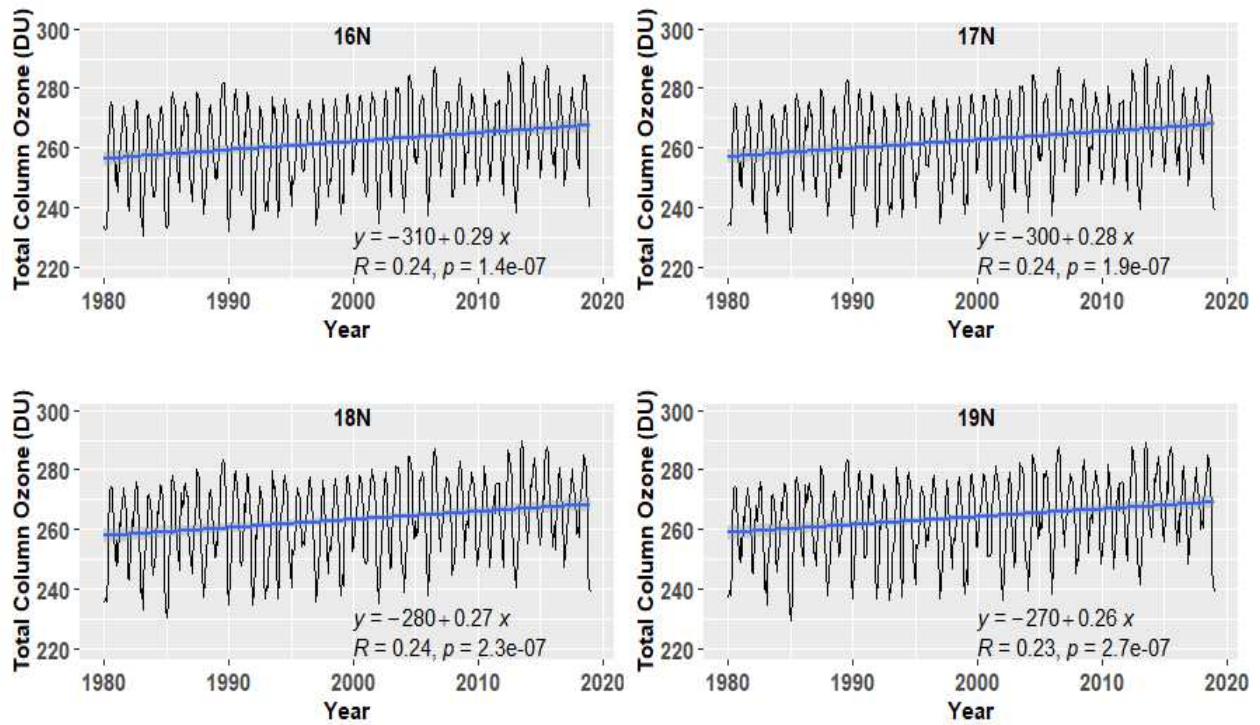
357

358



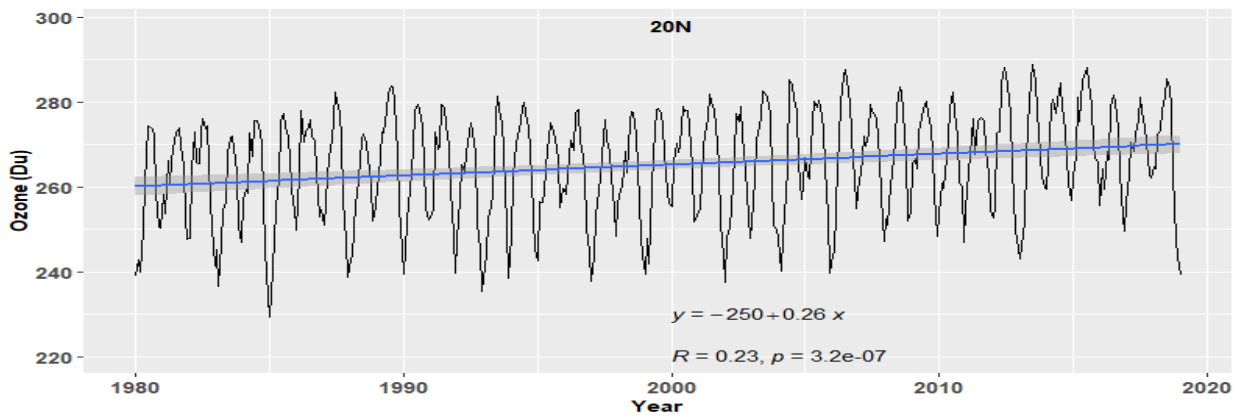
359

360 Fig. 13 Variation from 8-15⁰N



361
 362 **Fig. 14** Variation from 16-19⁰N

363
 364



365
 366 **Fig. 15** Variation at 20⁰N

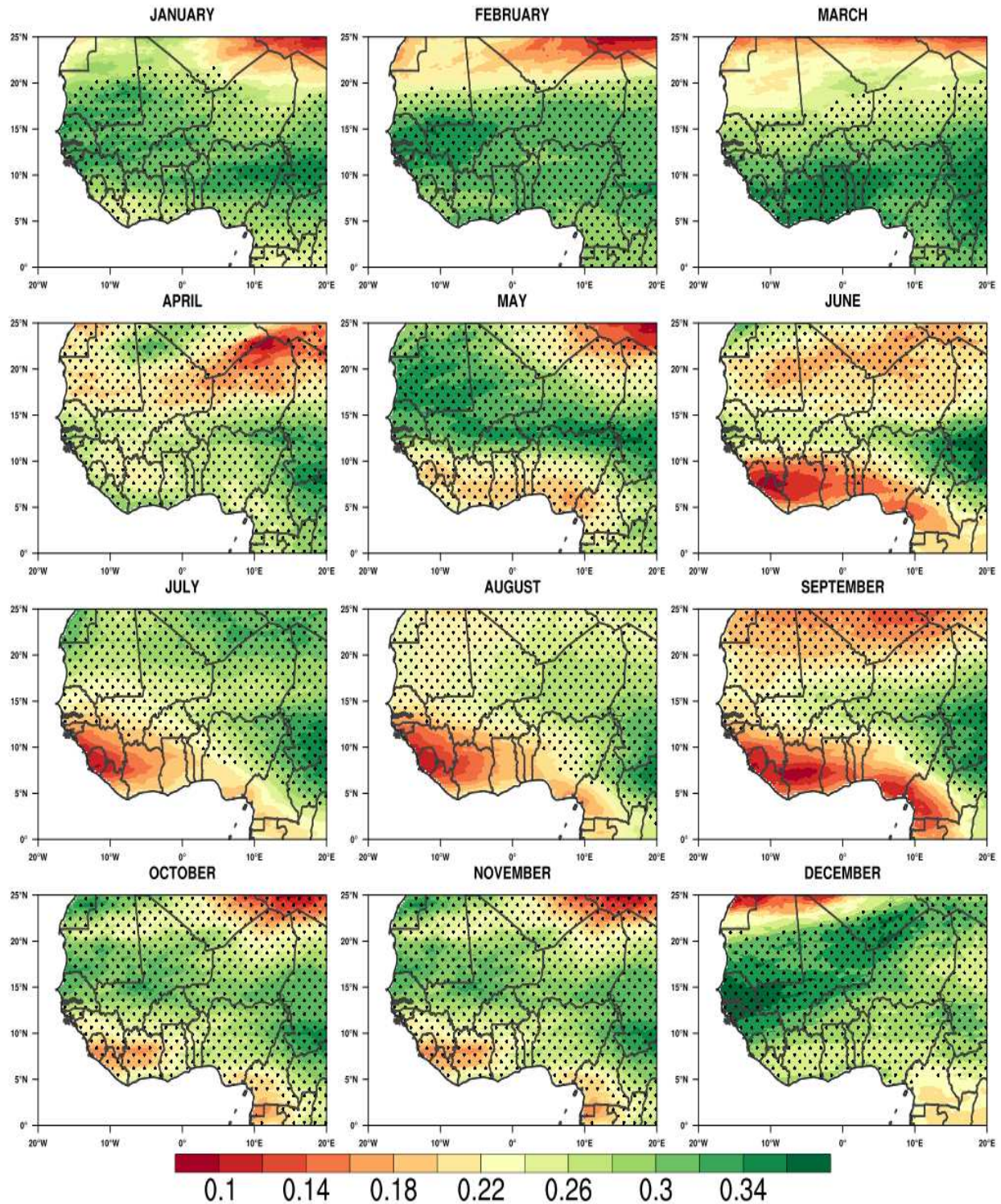
367
 368
 369
 370

371 **Table 2: Statistical Summary**

Latitude	Mean	Minimum	Maximum	Standard Deviation	TREND/YR	ACRV	Regression Coefficient
20 ⁰ N	265.20	229.30	289.00	12.39	0.20	4.28	0.227
19 ⁰ N	264.11	229.50	289.30	12.70	-0.98	4.41	0.228
18 ⁰ N	263.13	230.30	289.60	13.03	-0.99	4.55	0.227
17 ⁰ N	262.51	231.60	290.00	13.30	0.41	4.67	0.227
16 ⁰ N	261.98	230.60	290.20	13.50	3.07	4.77	0.231
15 ⁰ N	261.69	229.90	290.40	13.62	0.63	4.83	0.233
14 ⁰ N	261.58	229.40	290.60	13.65	0.99	4.84	0.239
13 ⁰ N	261.54	228.70	290.50	13.61	1.26	4.79	0.238
12 ⁰ N	261.42	227.90	290.10	13.49	1.48	4.75	0.237
11 ⁰ N	261.35	227.60	289.70	13.30	1.63	4.63	0.235
10 ⁰ N	261.74	228.00	289.20	13.03	1.81	4.51	0.240
9 ⁰ N	261.92	228.90	289.20	12.72	1.94	4.37	0.232
8 ⁰ N	261.96	229.90	289.70	12.40	11.71	4.24	0.231
7 ⁰ N	262.22	230.90	290.40	12.11	2.21	4.17	0.232
6 ⁰ N	262.58	232.50	291.60	11.88	2.39	4.14	0.238
5 ⁰ N	262.89	234.50	293.30	11.74	2.47	4.15	0.248
4 ⁰ N	262.92	235.90	295.00	11.65	2.60	4.18	0.261

372 .

373



374

375 **Fig. 16** Trend of Total column ozone over West Africa from 1980-2019; Region with black dots depict
 376 where the trend is significant at 95% confidence level.

377 The result of the Mann-Kendall (MK) trend analysis described by Mann (1945) and Kendall (1975) was
378 performed at 95% confidence level for the months over the study region. The result shows that, there is
379 an increasing trend over the months in the study area. With magnitude of change to be between 0.1 to
380 0.34. High magnitude was observed during the dry months and considerably low during the wet months.
381 High level of significance was observed in all the months, with the highest in November, which marks
382 the end of the wet season and the lowest in March. as observed in figure. 16 over the West Africa
383 region. In December, January, February and March, between latitude 20 to 25⁰N, the level of significant
384 is negligible and the trend over the area is also significantly low. While between latitude 4-20⁰N, the
385 trend is most positive over the region in these months. ITD position between these months is between
386 4-12⁰N. over these months the low significance level observed maybe attributed to the outlying position
387 of ITD. The tarrying months is in synchronization with the position of ITD over the region.

388 **CONCLUSION**

389 This study has examined and helped in understanding the influence of ITD on total column ozone over the
390 period between 1980–2019, over West Africa using satellite data. Both geospatial and correlation analyses
391 were performed to show variations in total column ozone and the influences of ITD over TCO in the period
392 of study. In this study, ITD is delineated to propagate between 4-20⁰N of the equator. The literature review
393 has provided an insight to the characterization, propagation and significant of ITD over West Africa based
394 on scientific literatures.

395 This study, on the other hand, has provided an update on the trend and connection between these two
396 distinct variables across the West African subcontinent. According to Oluleye and Okogbue (2013), there
397 are additional variables that regulate ozone concentration, with bush burning being the most important.
398 Bush burning is primarily responsible for the generation of photochemically reactive gases such as NO, CO,
399 and hydrocarbons, which combine to create ozone. The assumption is that the dry season is best for ozone
400 generation since there is apparently a lot of biomasses burning going on during this period.

401 This is not the situation over West Africa, which has the lowest ozone concentration during the dry season.
402 The footprints of the burnings were found to have a minor impact on the overall temporal and spatial
403 distribution of total column ozone. Oluleye and Okogbue (2013) attributed this to the fact that lower
404 atmospheric ozone is primarily controlled by bush burning, while ozone in the upper atmosphere is
405 independent of fluctuating lower atmospheric ozone concentrations, according to Combrink et al. (1995).
406 As a result, the total ozone distribution aligns in the direction of the upper atmospheric ozone control
407 mechanism, which happens to be the ITD over West Africa. The influence of ITD over west Africa is more

408 renowned during the dry months most especially in DJF that the wet months. However, lower
409 concentration is also observed in the dry months as opposed the wet months of JJA over the study region.
410 The major finding of this study is that TCO distributions vary over time and space, but there appears to be
411 a significance variation in the concentration of TCO along the ITD zone. Furthermore, the relationship
412 between ITD and TCO varies across latitudes but appears to be more significant between latitude 10-14°N,
413 which is the savannah region. it's also noted that throughout this study, ozone hole which is designated
414 by concentration less than or equal to 220DU was not recorded. The highest and lowest concentration was
415 295DU and 227.60DU respectively which gives a difference of about 67DU.

416

417 **Ethical Approval**

418 Not Applicable

419 **Consent for publication**

420 Not applicable

421 **Consent to Participate**

422 Not Applicable

423 **Competing Interest**

424 Authors have declared that there is no competing interest in this research.

425 **Authors Contribution**

426 Ayomide Arowolo and Ayodeji Oluleye both participated to the interpretation, data analysis and the review
427 of the manuscript.

428 **Funding**

429 The author(s) received no financial support for the research, authorship, and/or publication of this article.

430 **Acknowledgement**

431 The authors are grateful to Copernicus Climate Change Service (C3S) Climate Data Store for making the
432 datasets available on their website, which may be accessed via the European Centre for Medium-Range
433 Weather Forecasts (ECMWF). And to the Giovanni online data system, developed and maintained by the
434 NASA GES DISC. Many thanks also go to the reviewers who will be evaluating this manuscript; your
435 feedback will be immensely cherished.

436 **Data availability**

437 The datasets analysed during the current study are available at Giovanni at [https://giovanni](https://giovanni.gsfc.nasa.gov/giovanni/)
438 [.gsfc.nasa.gov/giovanni/](https://giovanni.gsfc.nasa.gov/giovanni/) and Era5 [https://cds.climate.copernicus.eu/cdsapp#!/dataset/reanalysis-era5-](https://cds.climate.copernicus.eu/cdsapp#!/dataset/reanalysis-era5-single-levels-monthly-means?tab=form)
439 [single-levels-monthly-means?tab=form](https://cds.climate.copernicus.eu/cdsapp#!/dataset/reanalysis-era5-single-levels-monthly-means?tab=form)

440 **References**

- 441 Adedokun, J.A., 1979. Towards achieving an in-season forecast of the West African precipitation.
442 Archivfür Meteorologie, Geo physik und Bioklimatologie Serie A 28, 19–38.
443
- 444 Aculinin, A. (2006) Variability of Total Column Ozone Content Measured at Chisinau Site, Republic of
445 Moldova. Moldavian Journal of Physical Science, 5, 240-248.
446
- 447 Adeyewa ZD, Oluleye A. Relationships between aerosol index, ozone, solar Zenith angle and surface
448 reflectivity: A case study of satellite observation over Lagos; 2011.
449
- 450 Akinyemi L. The influence of some atmospheric phenomena on total ozone over the tropics. Australian
451 Journal of Basic and Applied Science. 2007;1(4):497505.
452
- 453 Akinyemi, M.L. (2010). Total ozone as a stratospheric indicator of climate variability over West Africa.
454 International Journal of the Physical Sciences. 5(5), pp. 447-451
455
- 456 Allen J. (2004). Ozone and Climate Change. National Aeronautics and Space Administration (NASA), Earth
457 Observatory Release
458
- 459 Ayansina A., Godwin MA. Jegede O. Spatial and seasonal variations in atmospheric aerosols over Nigeria:
460 Assessment of influence of intertropical discontinuity movement The International Journal of
461 Ocean and Climate Systems. 2019; 1759313118820306
462
- 463 Bell, M. A., and P. J. Lamb, 2006: Integration of weather system variability to multidecadal regional climate
464 change: The West African Sudan–Sahel zone, 1951–98. J. Climate, 19, 5343–5365.
465
- 466 Bhattacharya, R. and Bhoumick, A. (2012) Trend Analysis of Total Column Ozone over India Using TOMS
467 Data from 1979 to 2010. International Journal of Engineering Science and Technology, 4, 2159-
468 2166.
469
- 470 Bou Karam, D., C. Flamant, P. Knippertz, O. Reitebuch, M. Chong, J. Pelon, and A. Dabas, 2008, Dust
471 emissions over the Sahel associated with the West African Monsoon inter-tropical discontinuity
472 region: a representative case study, Q. J. R. Meteorol. Soc. 134: 621–634.
473
- 474 Bou Karam D., C. Flamant, P. Tulet, M. C. Todd, J. Pelon and E. Williams, 2009a, Dry cyclogenesis and
475 dust mobilization in the Inter Tropical Discontinuity of the West African Monsoon: a case study,
476 Journal of Geophysical Research.
477
- 478 Bou Karam D., C. Flamant, P. Tulet, J-P. Chaboureau, A. Dabas, and M. C. Todd, 2009b, Estimate of
479 Sahelian dust emissions in the Intertropical discontinuity region of the West African Monsoon,
480 Journal of Geophysical Research.
481
- 482 Chen, D. L., Nunez, M., 1998. Temporal and spatial variability of total ozone in Southwest Sweden
483 revealed by two ground-based instruments. InternationalJournalofClimatology18,1237–1246.
484

485 Combrink, J., Diab, R.D., Sokolic, F., Brunke, E.G., 1995. Relationship between surface, free
486 tropospheric and total column ozone in two contrasting areas in South Africa. *Atmospheric*
487 *Environment* 29, 685–691.
488

489 Corlett, G.K., Monks, P.S., 2001. A comparison of total column ozone values derived from the Global
490 Ozone Monitoring Experiment (GOME), the Tiros Operational Vertical Sounder (TOVS), and the
491 Total Ozone Mapping Spectrometer (TOMS). *Journal of the Atmospheric Sciences* 58,1103–
492 1116.
493

494 C Dueñas, M.C Fernández, S Cañete, J Carretero, E Liger, Analyses of ozone in urban and rural sites in
495 Málaga (Spain), *Chemosphere*, Volume 56, Issue 6, 2004, Pages 631-639, ISSN 0045-6535,
496 <https://doi.org/10.1016/j.chemosphere.2004.04.013>.
497 <https://www.sciencedirect.com/science/article/pii/S0045653504002814>)
498

499 Citeau, J., L. Finaud, J. P. Cammas, and H. Demarcq, 1989: Questions relative to ITCZ migrations over
500 the tropical Atlantic Ocean, sea surface temperature and Senegal River runoff. *Meteor. Atmos.*
501 *Phys.*, 41, 181–190.
502

503 Diab, R.D., Thompson, A.M., Mari, K., Ramsay, L., Coetzee, G.J.R., 2004. Tropospheric ozone
504 climatology over Irene, South Africa, from 1990 to 1994 and 1998 to 2002. *Journal of*
505 *Geophysical Research–Atmospheres* 109, art.no. D20301.
506

507 Drobinski, P., S. Bastin, S. Janicot, O. Bock, A. Dabas, P. Delville, O. Reitebuch, and B. Sultan, 2009: On
508 the late northward propagation of the West African summer monsoon in summer 2006 in the
509 region of Niger/Mali. *J. Geophys. Res.*, 114, D09108, doi:10.1029/2008JD0011159.
510

511 Dunkerton, T.J., Delisi, D.P., 1985. Climatology of the equatorial lower stratosphere. *Journal of the*
512 *Atmospheric Sciences* 42,376–396.
513

514 Eldridge, R. H., 1957: A synoptic study of West African disturbance lines. *Quart. J. Roy. Meteor. Soc.*,
515 83, 303–314.
516

517 Fontain, B., and S. Janicot, 1992: Wind-field coherence and its variations over West Africa. *J. Climate*,
518 5, 512–524.
519

520 Grist, J.P., Nicholson, E., 2001. A study of the dynamic factors influencing the rain fall variability in the
521 West African Sahel. *Journal of Climate* 14, 1337–1359.
522

523 Grist, J.P., Nicholson, S.E., Barcion, A.I., 2002. Easterly waves over Africa. Part II: observed and
524 modelled contrasts between wet and dry years. *MonthlyWeatherReview* 130,212–225.
525

526 G. S. Meena & S. D. Patil (2011) Variation of total column ozone along the monsoon trough region over
527 north India, *International Journal of Remote Sensing*, 32:9, 2581-2590, DOI:
528 10.1080/01431161003698435.
529

530 Ilesanmi, O. O., 1971: An empirical formulation of an ITD rainfall model for the tropics: A case study of
531 Nigeria. *J. Appl. Meteor.*, 10, 882–891.

532
533 Ilori, O.W., Ajayi, V.O., 2020. Change detection and trend analysis of future temperature and rainfall over
534 west Africa. *Earth Syst. Environ.* 4 (3), 493–512. <https://doi.org/10.1007/s41748-020-00174-6>.
535
536 Jain, S.L., Kulkarni, P.S., Ghude, S.D., Polade, S.D., Arya, B.C. and Dubey, P.K. (2008) Trend Analysis of
537 Total Column Ozone over New Delhi, India. *MAPAN. Journal Metrology Society of India*, 23, 63-
538 69.
539 Kalita, G., Pathak, B., Bhuyan, P.K. and Bhuyan, K. (2011) Impact of Zonal Wind on Latitudinal Variation
540 of Total Columnar Ozone over the Indian Peninsula. *International Journal of Remote Sensing*,
541 32, 9509-9520. <https://doi.org/10.1080/01431161.2011.564221>
542 Kendall, 1975. *Rank Correlation Methods*, 4th edn. Charles Griffin, San Francisco, CA, p. 8.
543
544 Khan, N., et al., 2020. Spatiotemporal changes in precipitation extremes in the arid province of Pakistan
545 with removal of the influence of natural climate variability. *Theor.Appl.Climatol.* 142 (3–4), 1447–
546 1462. <https://doi.org/10.1007/s00704-020-03389-9>.
547
548 Kulkarni, P.S., Ghude, D.S., Jain, S.L., Arya, B.C. and Dubey, P.K. (2011) Tropospheric Ozone Variability
549 Over the Indian Coastline and Adjacent Land and Sea. *International Journal of Remote Sensing*,
550 32,1545-1559. <https://doi.org/10.1080/01431160903571825>
551
552 Lamb, P. J., 1978a: Case studies of tropical Atlantic surface circulation patterns during recent sub-
553 Saharan weather anomalies: 1967 and 1968. *Mon. Wea. Rev.*, 106, 482–491.
554
555 Lamb, P.J., 1978b: Large-scale tropical Atlantic surface circulation patterns associated with Sub-
556 Saharan weather anomalies. *Tellus*, 30, 240–251.
557
558 Lélé MI and Lamb PJ (2010). Variability of the Intertropical Front (ITF) and rainfall over the West African
559 Sudan-Sahel zone. *Journal of Climate*, vol. 23, no. 14, pp. 3984–4004.
560
561 Nicholson, S. E., 1980: The nature of rainfall fluctuations in subtropical West Africa. *Mon. Wea. Rev.*,
562 108, 473–487.
563
564 Nicholson, S.E., 2008: The intensity, location and structure of the tropical rain belt over West Africa as
565 factors in Interannual variability. *International Journal of climatology*, 28 (13): 1775-1785.
566
567 Nicholson, S.E., 2009: A revised picture of the structure of the “ monsoon” and land ITCZ over West
568 Africa. *Climate Dynamics*, 32(7-8): 1155-1171.
569
568 Nishanth, T., Praseed, K.M., Satheesh Kumar, M.K. and Valsaraj, K.T. (2014) Influence of Ozone Precursors
569 and PM10 on the Variation of Surface O3 over Kannur, India. *Atmospheric Research*, 138, 112-124.
570 <https://doi.org/10.1016/j.atmosres.2013.10.022>
571
571 Odumodu, L.O., 1983. Rainfall distribution, variability and probability in plateau–state, Nigeria. *Journal*
572 *of Climatology* 3, 385–393.
573
573 Ogunjobi K.O, Ajayi V.O, Balogun I.A., 2007. Long–term trend analysis of tropospheric total column
574 ozone in Africa. *Research Journal of Applied Science*2,280–284.

575 Olaniran, O.J., 1987. A study of the seasonal–variation of rain–days of different categories in Nigeria in
576 relation to the miller station types for tropical continents. *Theoretical and Applied Climatology*
577 38,198–209

578 Olsson L., 1983. Desertification or Climate? Investigation Regarding the Relationship Between Land
579 Degradation and Climate in the Central Sudan, University of Lund, Dept. of Physical Geography,
580 Sweden, pp.1–35.

581 Oluleye A, Okogbue EC. Analysis of temporal and spatial variability of total column ozone over West Africa
582 using daily TOMS measurements. *Atmospheric Pollution Research*. 2013; 4:387–397.
583

584 Oluleye A, Ogunjobi KO. The relationship of Nigerian rainfall to global teleconnections and sea surface
585 temperature *Journal of Meteorology and Climate Science*.2009; 8:71–83.
586

587 Omotosho, J.B., 1988.Spatial variation of rainfall in Nigeria during the 'little dry season'. *Atmospheric*
588 *Research* 22,137–147.

589 Omotosho JA and Abiodun BJ (2007). A numerical study of moisture build-up and rainfall over West Africa.
590 *Meteorological Applications*, 14(3):209–225.

591 Omotosho, J.B., 2008. Pre–rainy season moisture build–up and storm precipitation delivery in the
592 West African Sahel. *International Journal ofClimatology*28,937–946.

593 Pandey, R., & Vyas, B. (2004). Study of total column ozone, precipitable water content and aerosol optical
594 depth at Udaipur, a tropical station. *Current Science*, 86(2), 305–309. Retrieved March 5, 2021,
595 from <http://www.jstor.org/stable/24107872>

596 Peyrillé P and Lafore JP (2007). An idealized two-dimensional framework to study the West African
597 monsoon. Part II: Largescale advection and the diurnal cycle. *J. Atmos. Sci.*, 64, 2783–2803,
598 doi:10.1175/JAS4052.1.

599 Resmi, C.T., Nishanth, T., Satheesh Kumar, M.K., Balachandramohan, M. and Valsaraj, K.T. (2020) Long Term
600 Variation of Air Quality Influenced by Surface Ozone in a Coastal Site in India: Association with
601 Synoptic Meteorological Conditions with Model Simulations. *Atmosphere*, 11,
602 193.<https://doi.org/10.3390/atmos11020193>

603 Solomon, S., 1999. Stratospheric ozone depletion: a review of concepts and history. *Reviews of Geophysics*
604 37,275–316.

605 Stolarski, R.S., Bloomfield, P., Mcpeters, R.D., Herman, J.R., 1991. Total ozone trends deduced from Nimbus
606 7 TOMS data. *Geophysical ResearchLetters*18,1015–1018.

607 Sultan B and Janicot S (2000). Abrupt shift of the ITCZ over West Africa and intra-seasonal variability.
608 *Geophysical Research Letters*, vol. 27, no. 20, pp. 3353–3356.

609 Sultan B and Janicot S (2003). The West African monsoon dynamics. Part II: the “preonset” and “onset”
610 of the summer monsoon. *Journal of Climate* 16: 3389–3406.

611 Sultan B, Janicot S, and Diedhiou A (2003). The West African Monsoon dynamics. Part I: Documentation
612 of intra seasonal variability. *Journal of Climate*, 16 (21), 3389–3406.

- 613 Tohir, A.M., Portafaix, T., Sivakumar, V., Bencherif, H., Pazmino, A. and Begue, N. (2018) Variability and
614 Trend in Ozone over the Southern Tropics and Subtropics. *Annales Geophysicae*, 36, 381-404.
615 <https://doi.org/10.5194/angeo-36-381-2018>
- 616 World Meteorological Organization,1985. Atmospheric ozone: assessment of our understanding of the
617 processes controlling its present distribution and change. Its Global Ozone Research and
618 Monitoring Project, Report 1985 16, 1095.
- 619 World Meteorological Organization, Scientific Assessment of Ozone Depletion: 2018, Global Ozone
620 Research and Monitoring Project – Report No. 58, 588 pp., Geneva, Switzerland, 2018.
- 621 Xue Y., H. Juang, W.-P. Li, S. Prince, R. DeFries, Y. Jiao and R. Vasic, 2004, Role of land surface processes in
622 monsoon development: East Asia and West Africa, *J. Geophys. Res.*,109,
623 doi :10.1029/2003JD003,556.